Non-linear Spring-Mounted Flexible Plates in Axial Flow

R. M. Howell and A. D. Lucey

Abstract In this paper we model the fluid-structure interaction of non-linear flutter of a cantilever mounted upon a non-linear spring at the clamp in a uniform axial flow. This permits us to compare results with those from a *hybrid* non-linear system (a linear system mounted on a non-linear spring) and so to assess the change in fundamental physical phenomena owing to the introduction of full non-linear structural- and fluid-mechanics. We use numerical simulation for the non-linear system while our state-space solution of the corresponding linear system is used to guide the choice of parameters in the investigation. We show that above the flow speed of flutter-onset for small disturbances, amplitude growth leads to non-linear saturation so that the system settles into finite-amplitude oscillations. The frequencies of these oscillations evidence the dual-frequency characteristics of mount oscillation observed in physical experiments. When the natural frequency of the mount is low, we show that for a range of increases above the linear critical speed the linear hybrid and non-linear systems evidence the same frequency phenomena. However, the linear hybrid system evidences larger oscillation amplitudes than the non-linear system. Therefore, the stabilising effect of the non-linear structural terms outweighs the destabilising effect of the non-linear fluid terms.

1 Introduction

We model the fluid-structure interaction (FSI) of non-linear flutter of a cantilever of length L mounted upon a non-linear spring at the clamp in a uniform axial flow of speed U_∞. This system is depicted in Fig. 1. The fluid pressure is modelled using a non-linear potential flow method in the absence of a wake. This extends our linear study [1] that presented the stability space in the absence of damping and charted how the dynamics and the critical flutter velocity U_c at a mass ratio of $\bar{L} = 1$ depend

R. M. Howell (✉) · A. D. Lucey
Department of Mechanical Engineering, Fluid Dynamics Research Group, Curtin University of Technology, GPO Box U1987, Perth, WA 6845, Australia
e-mail: richard.howell@curtin.edu.au

Y. Zhou et al. (eds.), *Fluid-Structure-Sound Interactions and Control*, Lecture Notes in Mechanical Engineering,
https://doi.org/10.1007/978-981-10-7542-1_44

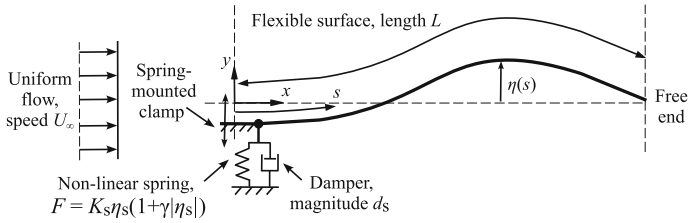

Fig. 1 The fluid-structure systems under consideration

upon the variation in natural frequency of the support of the spring-mass system ω_s. The non-linear spring stiffness is $K_s^* = K_s(1 + \gamma|\eta_s|)$ where γ is a constant that determines the magnitude of the non-linear stiffness contribution, as detailed in [2]. If simple dashpot damping d_s were to be included at the mount, the energy harvesting capabilities from the flutter instability could be measured and the fluid-structure system would then be classified as a type of *flutter mill*, for example see [3].

2 Method

The non-linear Euler-Bernoulli beam equation is presented in [3]. The modified version for the system illustrated in Fig. 1 is

$$\begin{aligned} -\delta p \;=\; & \rho h \frac{\partial^2 \eta}{\partial^2 t} - \rho h \frac{\partial \eta}{\partial s} \int_0^s \left(\left(\frac{\partial^2 \eta}{\partial t \partial s} \right)^2 + \frac{\partial \eta}{\partial s} \frac{\partial^3 \eta}{\partial t^2 \partial s} \right) \mathrm{d}s \\ & - \rho h \frac{\partial^2 \eta}{\partial s^2} \int_s^L \int_0^s \left(\left(\frac{\partial^2 \eta}{\partial t \partial s} \right)^2 + \frac{\partial \eta}{\partial s} \frac{\partial^3 \eta}{\partial t^2 \partial s} \right) \mathrm{d}s\mathrm{d}s \\ & + B \left[\frac{\partial^4 \eta}{\partial s^4} + \frac{\partial^4 \eta}{\partial s^4} \left(\frac{\partial \eta}{\partial s} \right)^2 + 4 \frac{\partial \eta}{\partial s} \frac{\partial^2 \eta}{\partial s^2} \frac{\partial^3 \eta}{\partial s^3} + \left(\frac{\partial^2 \eta}{\partial s^2} \right)^3 \right] + d_s \frac{\partial \eta_s}{\partial t} + K_s^* \eta_s. \end{aligned} \tag{1}$$

B, ρ and h are respectively the flexural rigidity, material density and thickness of the plate. The plate is discretised into N mass points spaced $\delta s = L/N$ apart where s is the ordinate along the plate. This derivation is based upon the assumption that the plate is inextensible *i.e.* L does not vary and therefore δs is constant. At the downstream end of the plate, conditions of zero bending moment and shear are applied. To enforce a spring-mounted clamp at the upstream end of the plate, the leading edge of the plate must follow the heaving motion of the actuating force from the clamp. These constraints are applied through a *shear-force balance*, as detailed in [1], which couples the plate dynamics to the motion of the spring-mount. This also permits the plate to drive the motion of the mount. A final condition of zero gradient at the leading edge of the plate completes the imposition of the spring-mounted clamp. Finally,

Table 1 Mount oscillation frequencies for increasing $\bar{U}$ with $\bar{\omega}_s = \bar{L} = 1$ and $\bar{\gamma} = 1 \times 10^4$

	Linear			Non-linear		
Δ	$\bar{\omega}_L$	$\bar{\omega}_U$	I_U	$\bar{\omega}_L$	$\bar{\omega}_U$	I_U
0.6	11.1	33.4	0.18	10.6	32.1	0.15
0.8	11.3	34.1	0.20	10.9	32.6	0.17

the last two terms on the right-hand side of Eq. (1) account for damping and spring stiffness at the mount.

The fluid modelling is based on the non-linear boundary-element method detailed in [4] that modelled the non-linear FSI of flow over one side of a flexible, simply supported plate. The plate is discretised into N panels each of length δs, the centre of which coincide with the mass points described above. The non-linear vortex strengths for each panel are found through the no-flux condition, $\{\gamma\} = [I^N]^{-1}\{U_\infty \sin\theta + \dot{\eta}\cos\theta - \dot{\xi}\sin\theta\}$, where θ is the angle of each panel on the plate with respect to the horizontal and $\dot{\xi}$ and $\dot{\eta}$ are the velocities of each panel in the x- and y-directions respectively. This equation is used to solve for the flow field. This is then inserted into the unsteady Bernoulli equation to determine the transmural pressure difference across the plate of $-\delta p = \delta p' + \rho_f[\mathbf{B}_2]\ddot{\eta}\cos\theta$, where $\delta p'$ summarises 10 pressure terms that do not depend on $\ddot{\eta}$, $[\mathbf{B}_2]$ is a matrix that contains the influences of the panels on each other and ρ_f is the density of the free-stream fluid. This pressure formulation is combined with Eq. (1) to generate an equation for the full fluid-structure system in terms of $\ddot{\eta}$ that is solved using a time-stepping, semi-implicit method of solution; this type of initial-value solution is fully detailed in [4].

3 Results

Following [2], results are non-dimensionalised using reference length and time scales $L_r = \rho h/\rho_f$ and $t_r = (\rho h)^{\frac{5}{2}}/(\rho_f^2 B^{\frac{1}{2}})$ respectively. In [2], values of oscillation frequency $\bar{\omega} = \omega t_r$ were obtained of the mount- and tip-oscillation displacement in the absence of damping for the FSI of the hybrid system. These are presented on the left-hand side in the first row of Table 1 for $\Delta = 0.6$ above the linear flutter-onset flow speed U_c (*i.e.* $U_\infty = U_c(1 + \Delta)$) with $\bar{L} = L/L_r = 1$ and $\bar{\omega}_s = \omega_s t_r = 1$. The value $\bar{\gamma} = \gamma L_r$ is set to an illustrative value of 1×10^4. These results show that there are two different frequencies present in the time series of the mount oscillation. The term I_U is the intensity of the higher frequency divided by the intensity of the lower frequency. It can therefore be seen that the lower frequency, associated with single-mode flutter, dominates the oscillation. Its frequency is close to that for the corresponding fixed cantilever at 15.3. The higher frequency is close to the third mode *in vacuo* of the spring mounted cantilever. The equivalent $\Delta = 0.6$ results for

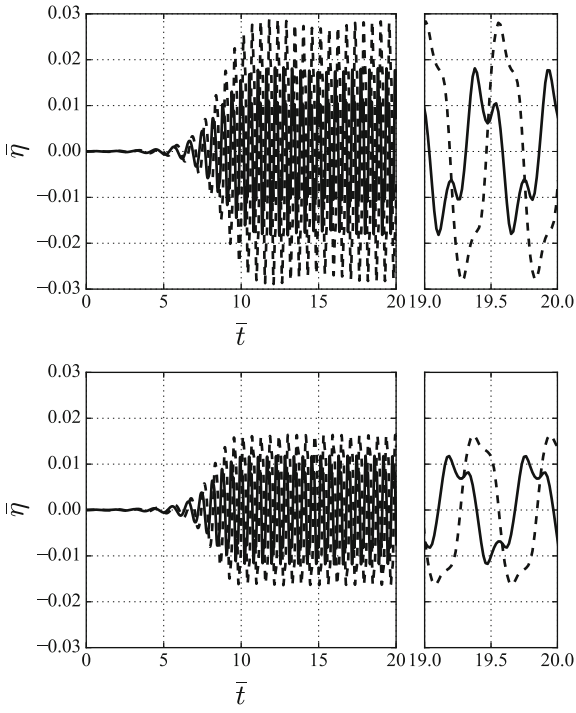

Fig. 2 Displacement in time for $\Delta = 0.8$ with $\bar{\omega}_s = \bar{L} = 1$ and $\bar{\gamma} = 1 \times 10^4$:—Mount, - - Tip. Plate and fluid mechanics: Top - linear, Bottom - non-linear. Small windows show traces from $\bar{t} = 19$ to 20

the non-linear cantilever are shown on the right-hand side in the first row of Table 1: little difference is seen as amplitudes are of a magnitude for which linear mechanics still hold. As shown in the second row of Table 1, similar frequency phenomena are found at $\Delta = 0.8$.

However, there is a difference in displacements. In Fig. 2 we plot $\bar{\eta} = \eta / L_r$ against $\bar{t} = t/t_r$ for the cantilever mount and tip displacements for $\Delta = 0.8$. The similarity of the frequency properties between the bybrid and non-linear models are shown by the mount–and tip-traces in the windows from $\bar{t} = 19$ to 20 on the right-hand side of Fig. 2. The left-hand side figures show that although both systems saturate by $\bar{t} = 10$ for a similar rate of amplitude increase, clearly the final amplitude magnitudes differ, the non-linear system amplitude smaller by a third. Therefore, the stabilising effect of the non-linear structural terms outweighs the destabilising effect of the non-linear fluid terms *i.e.* as displacement increases, the non-linear plate mechanics increase their stiffness non-linearly whereas the fluid forces continue to increase nearly linearly.

Mount and tip amplitudes for a range of Δ are shown in Fig. 3. In both cases, with increasing Δ tip displacement grows at a larger rate than mount displacement. For the non-linear case, the hysteresis loop has reduced in size, now only extending to $\Delta = -0.1$ whereas the linear loop extends to $\Delta = -0.2$.

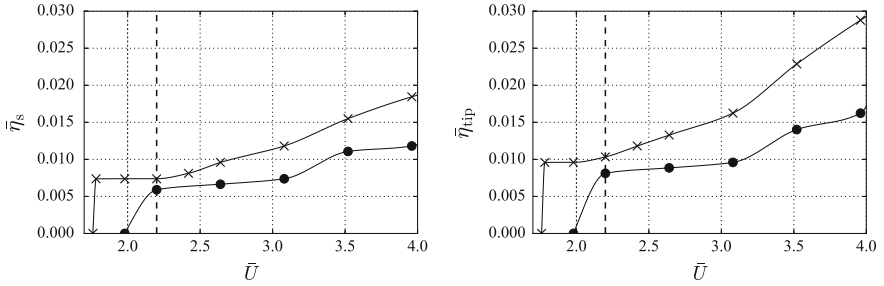

Fig. 3 Maximum displacement for increasing $\bar{U}$ with $\bar{L} = 1$, $\bar{\gamma} = 1 \times 10^4$ and $\bar{\omega}_s = 1$: The vertical dashed lines denote U_c for the linear case. Plate and fluid mechanics: × linear, • non-linear. Left: mount, Right: tip

4 Conclusions

We have presented a model for predicting the two-dimensional stability characteristics of non-linear, spring-mounted cantilevered plates in a uniform flow. The dynamics of the system have been investigated for cases that, for a rigid mounting, would succumb to single-mode flutter at instability onset. In the hybrid system, a non-linear spring at the mount permits dual frequency mount oscillation and saturation of this oscillation with increasing amplitude for increasing flow speed above the linear U_c. The value of the main, low frequency, component of the response lies between the natural frequency of the mount $\bar{\omega}_s$ and the frequency at flutter onset of a fixed cantilever; the higher frequency is close to the third mode *in vacuo* of the spring mounted cantilever.

When the natural frequency of the mount is low, we show that above the linear critical speed the linear hybrid and non-linear systems evidence the same frequency phenomena; however, the mount and tip displacement of the non-linear model is much smaller as the stabilising effect of the non-linear structural terms outweighs the destabilising effect of the non-linear fluid terms. This effect leads to a reduction in the size of the hysteresis loop.

Immediate future work will investigate a range of mount natural frequencies. The inclusion of the effect of the substantial wake that must form at the flow separation point will then be quantified through the inclusion of a discrete-vortex model, similar to the method described in [5]. It is finally noted that the non-linear model will be able to continue to grow to much larger amplitudes at higher values of Δ which augurs well for energy harvesting applications.

References

1. Howell RM, Lucey AD (2015) Flutter of spring-mounted flexible plates in uniform flow. J Fluids Struct 59:370–393

2. Howell RM, Lucey AD (2016) Flutter of a nonlinear-spring-mounted flexible plate for applications in energy harvesting. In: 20th Australasian fluid mechanics conference, Dec 5–8, Perth, Australia
3. Tang L, Paidoussis MP, Jiang J (2009) Cantilevered flexible plates in axial flow: Energy transfer and the concept of flutter mill. J Sound Vib 326:529–542
4. Lucey AD, Cafolla GJ, Carpenter PW, Yang M (1997) The nonlinear hydroelastic behaviour of flexible walls. J Fluids Struct 11:717–744
5. Howell RM, Lucey AD, Carpenter PW, Pitman MW (2009) Interaction between a cantilevered-free flexible plate and ideal flow. J Fluids Struct 25:544–566